

## Supplemental Data

### Somatic Mutations in *TSC1* and *TSC2*

#### Cause Focal Cortical Dysplasia

Jae Seok Lim, Ramu Gopalappa, Se Hoon Kim, Suresh Ramakrishna, Minji Lee, Woo-il Kim, Junho Kim, Sang Min Park, Junehawk Lee, Jung-Hwa Oh, Heung Dong Kim, Chang-Hwan Park, Joon Soo Lee, Sangwoo Kim, Dong Seok Kim, Jung Min Han, Hoon-Chul Kang, Hyongbum (Henry) Kim, and Jeong Ho Lee

## Supplemental figures

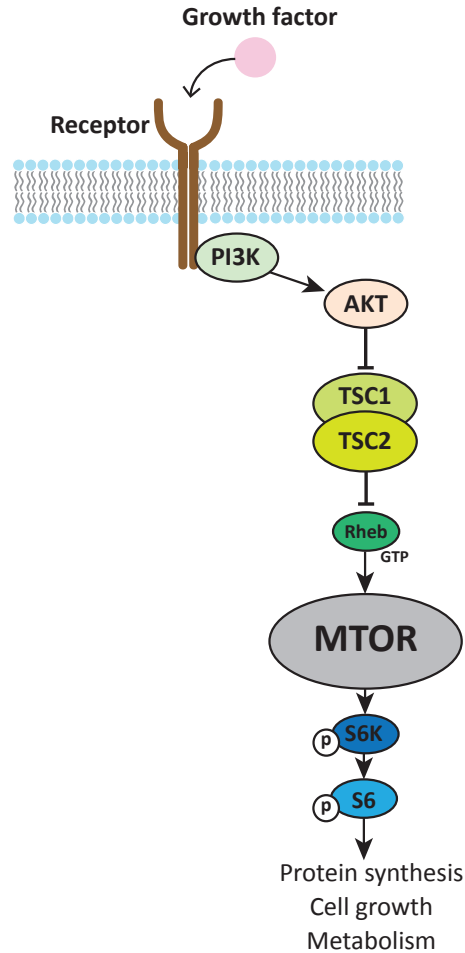
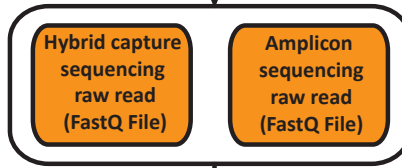


**Figure S1.** Schematic figure of the PI3K-AKT-TSC-mTOR pathway.

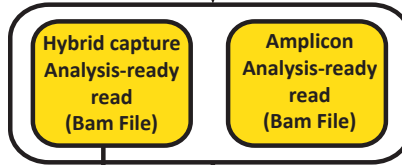
The PI3K-AKT-TSC-mTOR pathway, including downstream phosphorylated ribosomal protein S6 kinase (P-S6K) and phosphorylated ribosomal protein S6 (P-S6), is presented. The *PIK3*, *AKT* and *TSC* genes encode well-known regulators of the mTOR signaling. The TSC1/TSC2 complex regulates mTOR activity via hydrolysis of Rheb-GTP protein. P-S6K and P-S6 protein are the major readout of mTOR pathway activation in protein synthesis, cell growth and metabolism.

Pre-processing

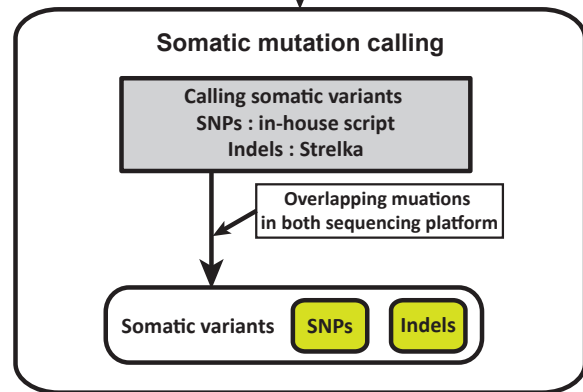
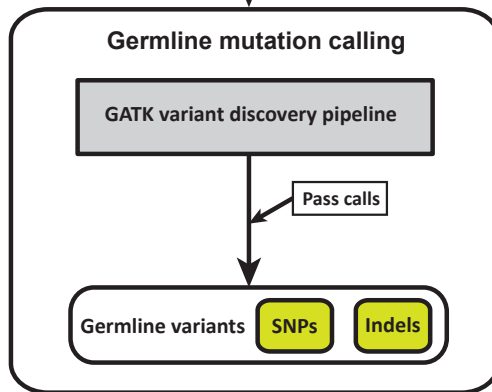
Design the panel for targeted sequencing of 5 mTOR pathway genes (*PIK3CA*, *PIK3R2*, *AKT3*, *TSC1*, *TSC2*)



Map to Reference(GATK best practice)  
Hybrid capture : with deduplication process  
Amplicon sequencing : without deduplication process



Variant Discovery



Variant evaluation

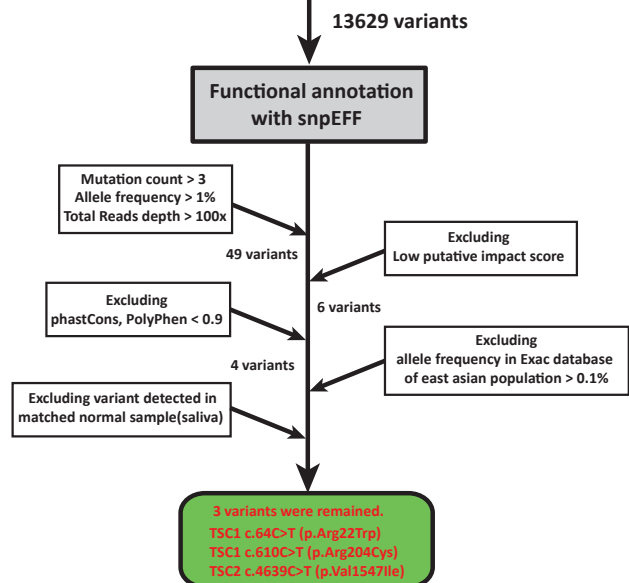
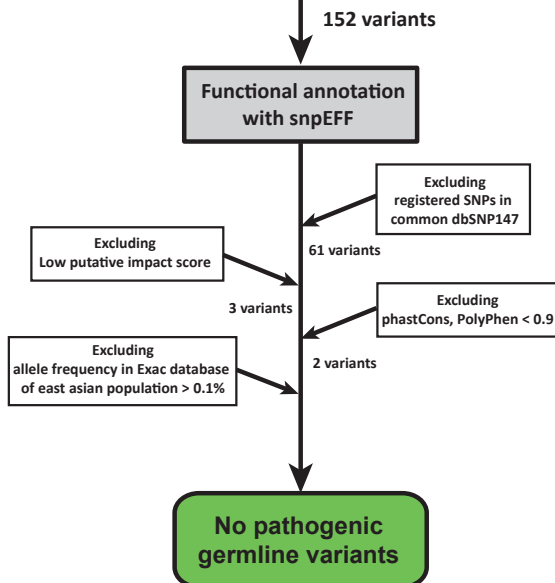
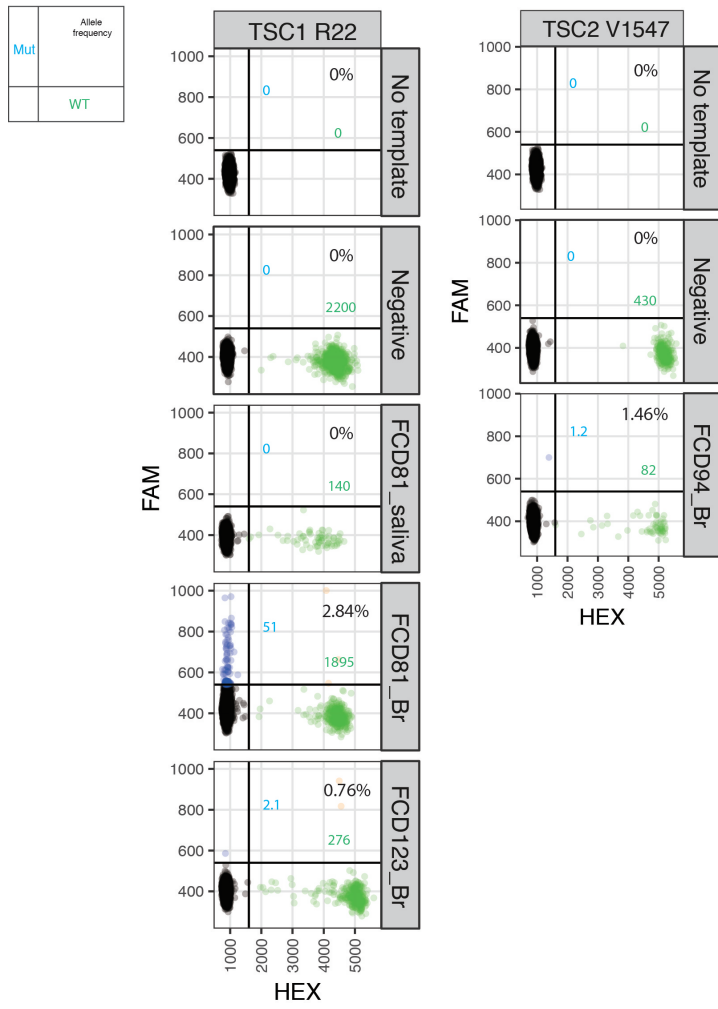


**Figure S2.** Schematic diagram of the bioinformatics pipeline to analyze the targeted deep sequencing data from 5 mTOR pathway genes.

(A) Data for the raw reads data qualified with FastQC was mapped to their correct genomic sequence and analysis-ready reads were analyzed to identify germline and somatic mutations. Because the PCR-based sequencing contained many duplicated reads, we modified the GATK pipeline to exclude deduplication process for mapping the the raw amplicon reads. We used hybrid capture data for the germline calling process. We then excluded 1) registered mutations in the public database (common dbSNP147); 2) mutations with a putative low impact score; 3) mutations with a PolyPhen score <0.9 and phastCons score <0.9; and 4) mutations with allele frequency in ExAC database of east asian population > 0.1%. As a result, No pathogenic germline mutations were found. Somatic single nucleotide variations and indels were called using an in-house script and strelka, respectively. Analysis ready bam files were converted to pileup files using SAMtools (<http://samtools.sourceforge.net>) and called for mutation/reference count using customized python script. Next, we called the overlapping mutations from both sequencing platforms and annotated the mutation using the snpEFF program.<sup>1</sup> We then excluded 1) mutations with a mutant read <4, allele frequency <1% and total read depth < 100 ×-to remove erroneous calls; 2) mutations with a putative low impact score; 3) mutations with a PolyPhen score <0.9 and phastCons score <0.9; and 4) mutations with allele frequency in ExAC database of east asian population > 0.1%. 5) mutations detected in matched peripheral samples (e.g. saliva). As a result, three mutations were remained for functional validation.

**A**

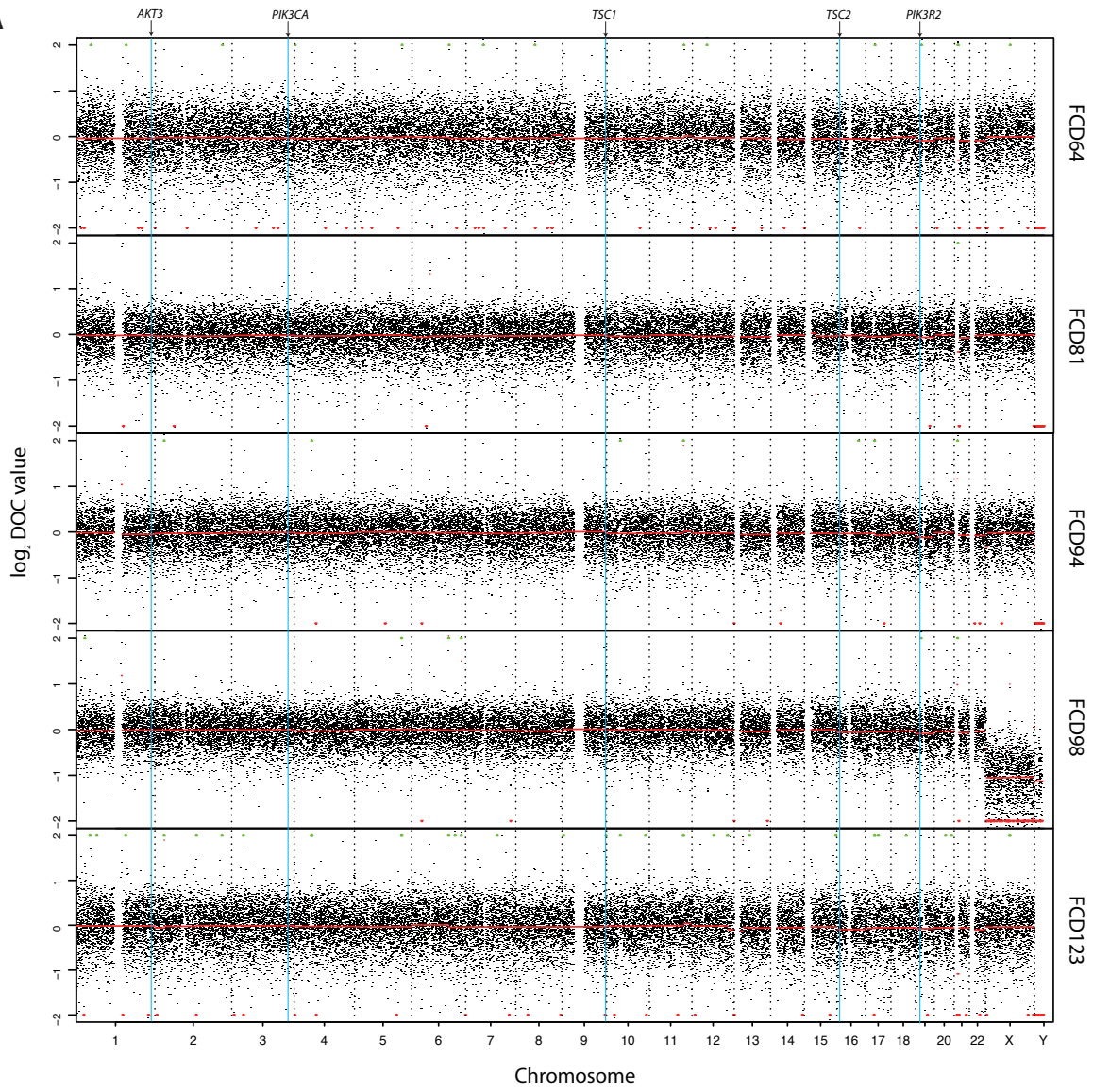
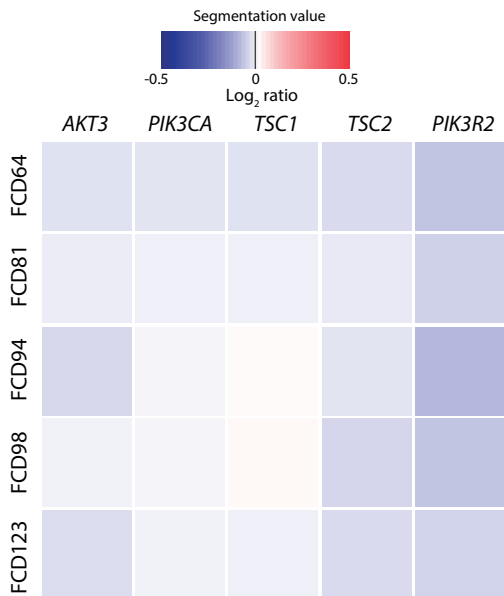


**B**



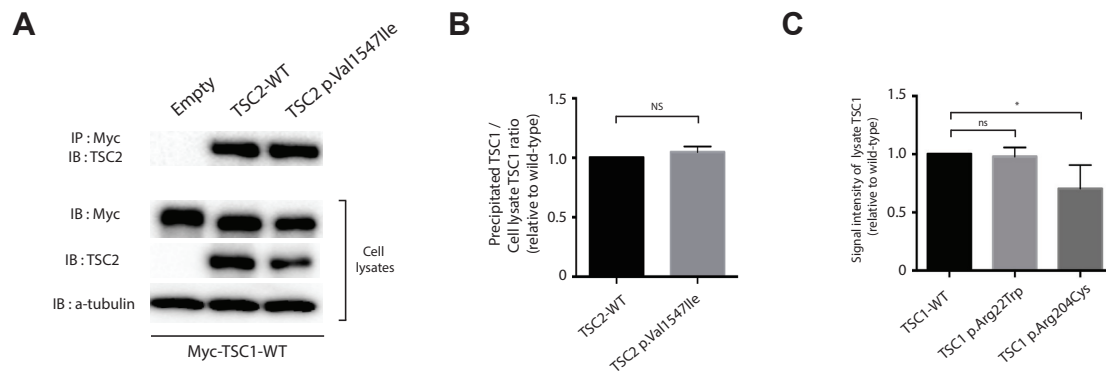
**Figure S3.** Identified somatic mutations were confirmed by droplet digital PCR (ddPCR) and ultra-high depth amplicon sequencing.

(A) Mutant-specific (FAM, blue signal) and wild-type-specific (HEX, green signal) locked nucleic acid (LNA) probes targeting the site of TSC1 R22 and TSC2 V1547 were used. FAM and HEX signal threshold were determined using no DNA template group ('No template'). Genomic DNA extracted from saliva of healthy individual was used as negative control ('Negative'). Blue or green numbers shown in the plots represent the copy number of mutant or wild-type positive signal calculated by Quantasoft program, respectively. Mut, mutant, WT, wild-type. (B) Visualization of the identified brain somatic mutations in deep amplicon sequencing. Arrow indicate the target locus in integrated genomic view (collapsed mode) of aligned sequencing file. Observed allele frequency of deep sequencing are calculated by dividing altered allele count by total allele count. NA, not available, Alt, altered.

**A****B**

**Figure S4.** No germline CNVs were detected in the individuals carrying *TSC1* or *TSC2* somatic mutations. (A) To detect germline CNVs in 5 individuals carrying somatic mutation on *TSC1* or *TSC2*, targeted panel sequencing data of these individuals were analyzed using copywriteR.<sup>2</sup> We calculated the number of reads that map to genome-wide consecutive 100 kb windows (bins) to generate the depth of coverage (DOC). No definitive large CNV were detected in genome-wide scale. Blue lines indicate the target sites of gene panel including *AKT3*, *PIK3CA*, *TSC1*, *TSC2*, *PIK3CA*. Segmentation values depicted in red. (B) Segmentation values of 5 individuals on the site of target genes were represented as heatmap.

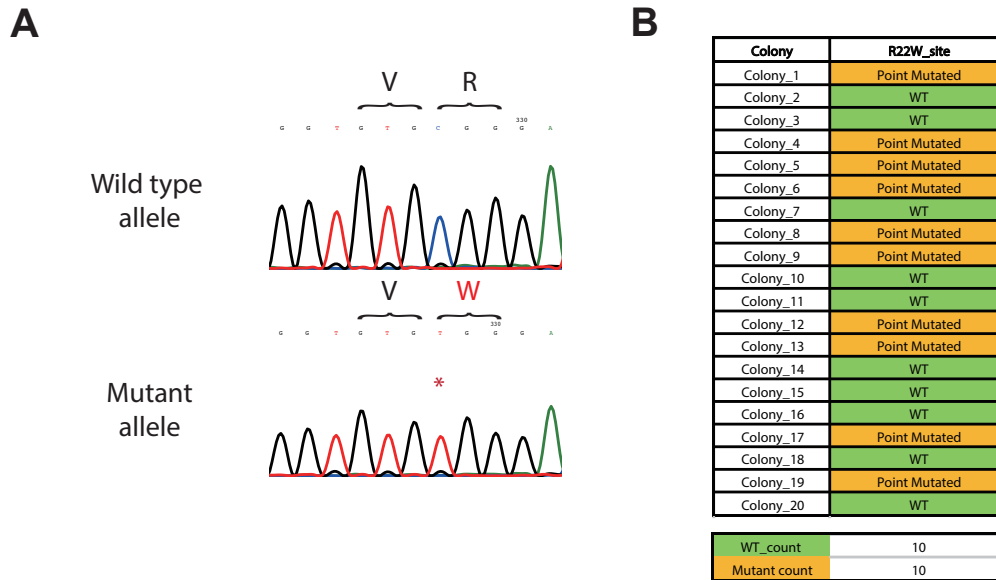




**Figure S5.** Immunoprecipitation assay of mutant TSC2 protein and wild type TSC1 protein and quantification of the expression of wild type and mutant TSC1 protein in **Figure 2D**.

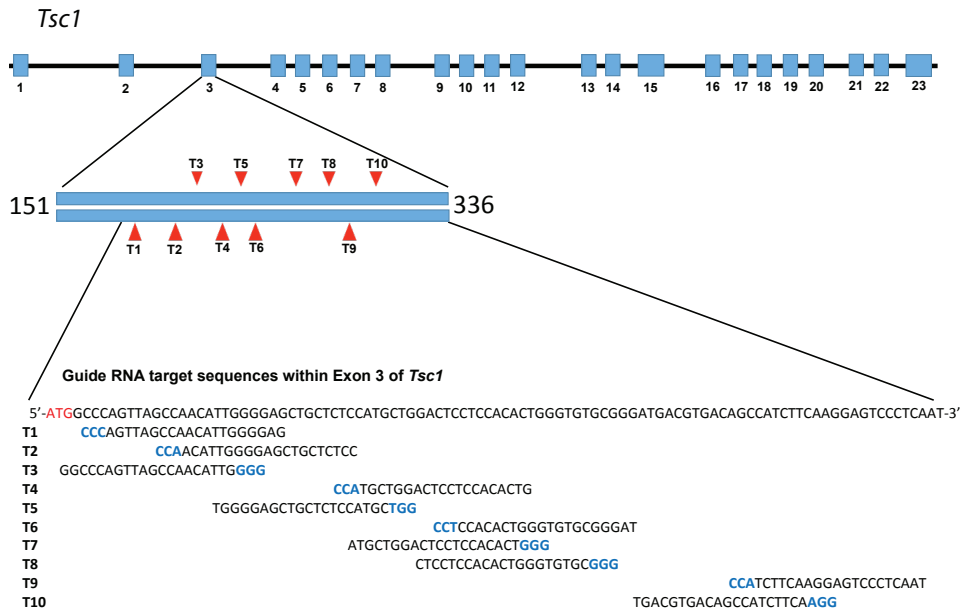
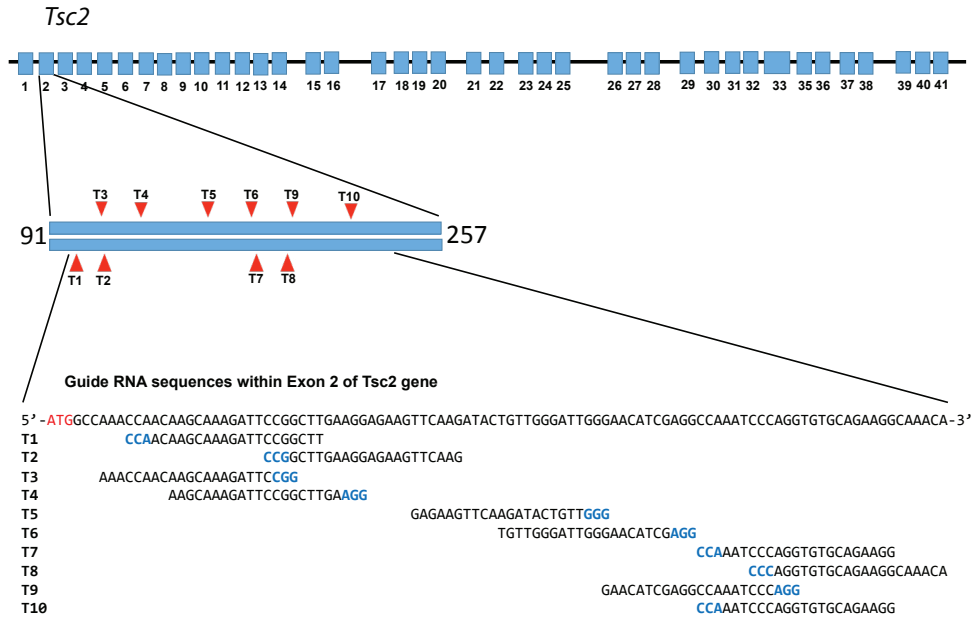
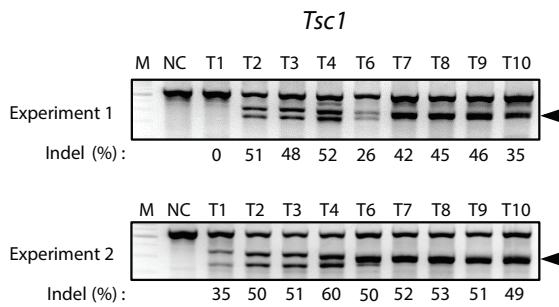
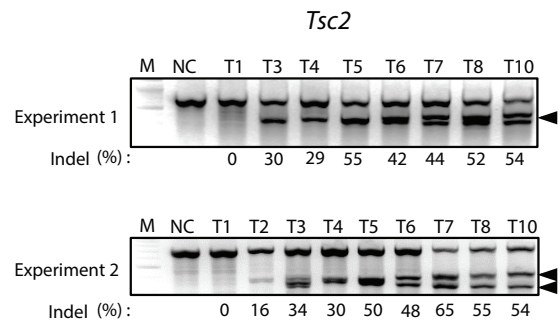
(A) HEK293T cells were transiently co-transfected with myc-tagged wild-type TSC1 and flag-tagged wild-type TSC2 or mutant TSC2. Lysates were immunoprecipitated with anti-myc antibody and immunoblotted with anti-TSC2 antibody. (B) Quantification of the TSC1 blotting intensity immunoprecipitated with TSC2 antibody. Data are the mean  $\pm$  SEM (n=4 per group). Student's t-test, compared with wild-type. NS, no significant difference. (C) Quantification of the expression of wild type and mutant TSC1 protein in **Figure 2D**. Data are the mean  $\pm$  SEM (n=4 per group). \* $P$ <0.05 compared with wild type, Student's t-test. WT, wild type; ns, not significant.

Generation of monoallelic N2A cell line carrying Tsc1 p.Arg22Trp



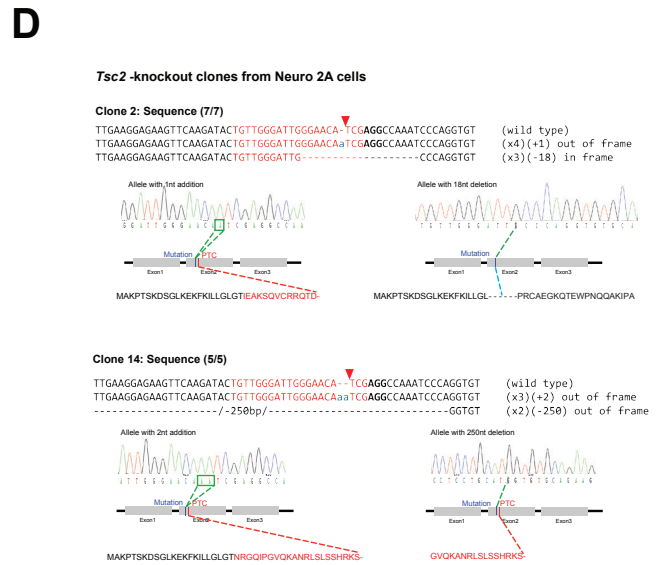
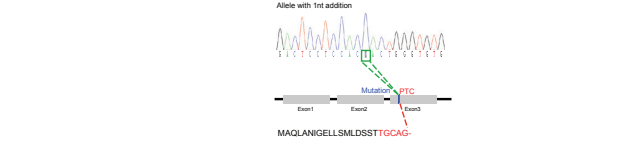
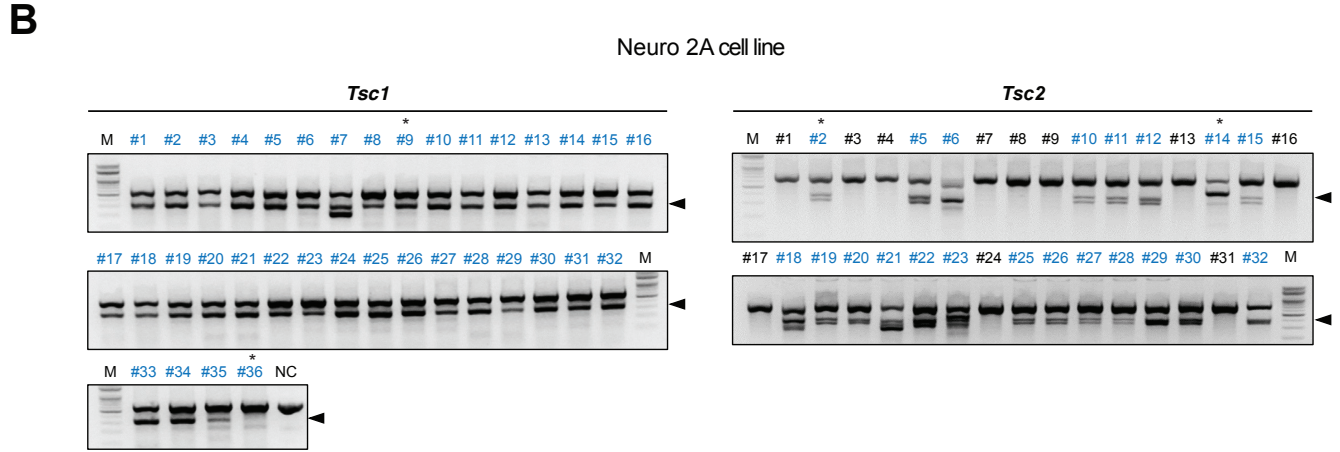
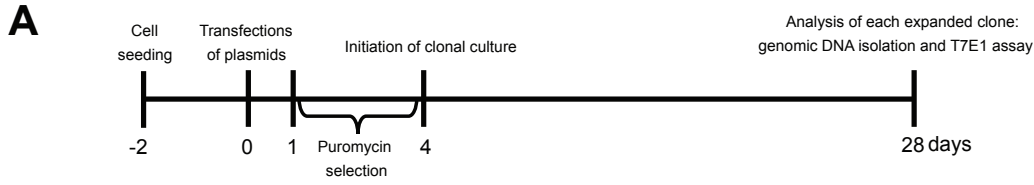
**Figure S6.** Generation of Neuro2A cell line carrying monoallelic TSC1 p.Arg22Trp mutation.

(A) The Sanger sequencing of TSC1 Arg22 site from wild-type and mutant colony, which were subcloned from Neuro2A cell line with monoallelic TSC1 p.Arg22Trp mutation. The single point mutation (red asterisk) was generated. It resulted in single amino acid substitution observed in individuals with FCD. V, Valine; R, Arginine; W, Tryptophan. (B) The subcloning and subsequent colony sequencing result of TSC1 p.Arg22 site. The number of wild-type and mutant colony was counted. The result shows that the established Neuro2A clone contain monoallelic TSC1 p.Arg22Trp mutation (heterozygous mutation).

**A****B****C****D**

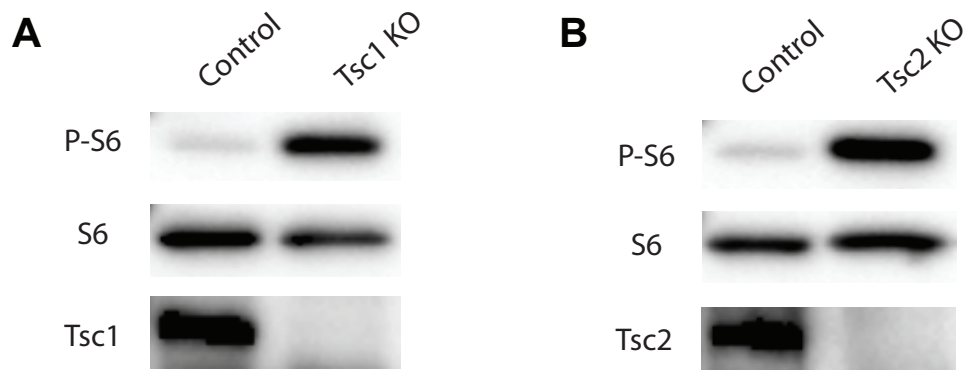
**Figure S7.** Selection of sgRNAs targeting the mouse *Tsc1* and *Tsc2* genes.

(A-B) Schematic of the Cas9-targeting sites in the mouse *Tsc1* (A) and *Tsc2* (B) locus with the designed sgRNAs (T1-T10) targeting sequences in exon 3 of *Tsc1* (A) or exon 2 of *Tsc2* (B). Blue boxes represent exons. Red arrowheads indicate the position of the sgRNA targeting top (T1, T2, T4, T6, and T9 for *Tsc1*; T1, T2, T7 and T8 for *Tsc2*) and bottom (T3, T5, T7, T8, and T10 for *Tsc1*; T3, T4, T5, T6, T9 and T10 for *Tsc2*) strands. PAM sequences are indicated in bold blue fonts. (C-D) The cleavage efficiency of sgRNAs targeting *Tsc1* (C) and *Tsc2* (D) were determined using T7E1 assays in Neuro2A cells following transfection with plasmids encoding Cas9 and sgRNAs. The results of two independent experiments are shown. The size markers (M) are shown on the left. Arrowheads indicate the expected positions of the DNA bands cleaved by T7E1. The numbers at the bottom of the gel indicate mutation percentages measured by band intensities. Untransfected cells served as the negative control (NC).



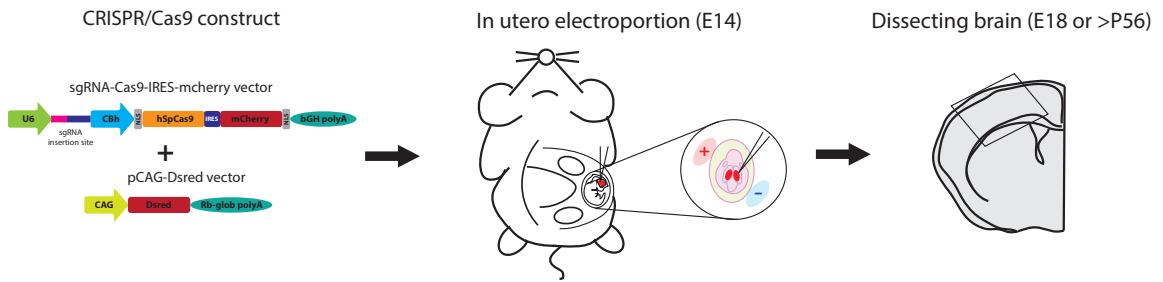
**Figure S8.** Generation of *Tsc1*- and *Tsc2*-mutated Neuro2A cell lines.

(A) Schematic representation illustrating the process used to generate clones carrying the *Tsc1*- and *Tsc2*-mutation. Clonal culture of Neuro2A cells was initiated 4 days after transfection with plasmids encoding Cas9 and sgRNAs targeting *Tsc1* and *Tsc2*. Transfected cells were enriched by puromycin treatment for 3 days. Genomic DNA from each clone was analyzed 24 days after the initiation of the clonal culture. (B) T7E1-based clonal analysis. The genomic DNA isolated from each clone was subjected to the T7E1 assay. Arrowheads indicate the expected position of the DNA bands cleaved by T7E1. Untransfected cells served as the negative control (NC). Clones that were successfully cleaved by T7E1 are indicated in blue font. M, size markers. (C-D) The *Tsc1* gene sequences from Neuro2A clones containing heterozygous (clone #9) and homozygous (clone #36) biallelic mutations in exon 3 (C). The *Tsc2* gene sequences from Neuro2A clones containing heterozygous biallelic mutations in exon 2 (D). The sgRNA recognition sites and protospacer adjacent motif are shown in red and bold font, respectively. Deleted bases are indicated by dashes, and inserted bases are shown in a small blue font. The number of occurrences is shown in parentheses (for example, × 4 and × 8 indicate the number of each sequence). The number of deleted and inserted bases is described in the parentheses on the right. The sequence and sequencing chromatogram for each allele are shown. The locus of each mutation and the premature termination codon (PTC) generated by the mutation are depicted in schematics of the *Tsc1* or *Tsc2*. Red arrowheads indicate the Cas9 cleavage sites. Clones that contain frame-shifting biallelic mutations without wild type alleles (clone 36 as TSC1 knockout cells and clone 14 as TSC2 knockout cells) were used in the subsequent studies as *Tsc1*- or *Tsc2*-knockout cells.



**Figure S9.** Hyperactivation of the mTOR pathway in *Tsc1*- and *Tsc2*-mutated Neuro2A cells.

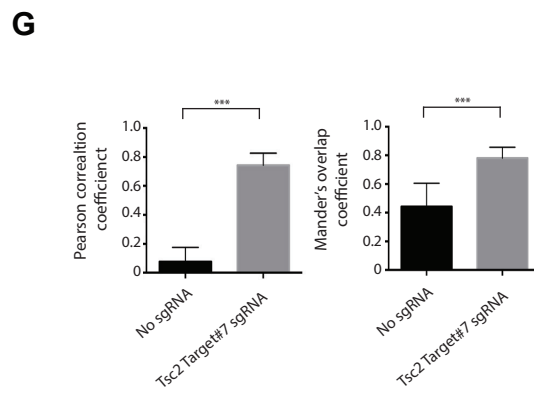
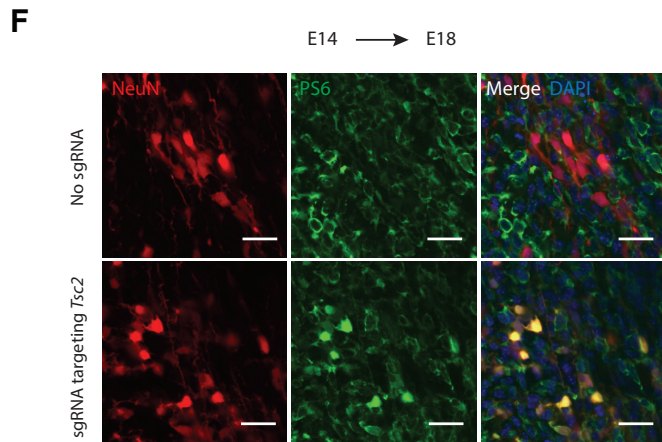
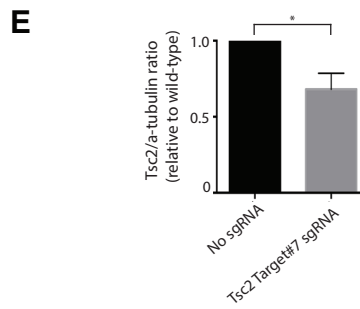
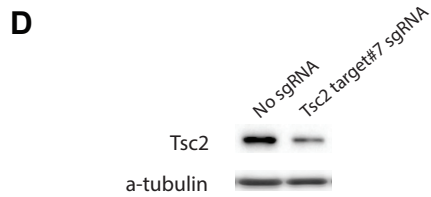
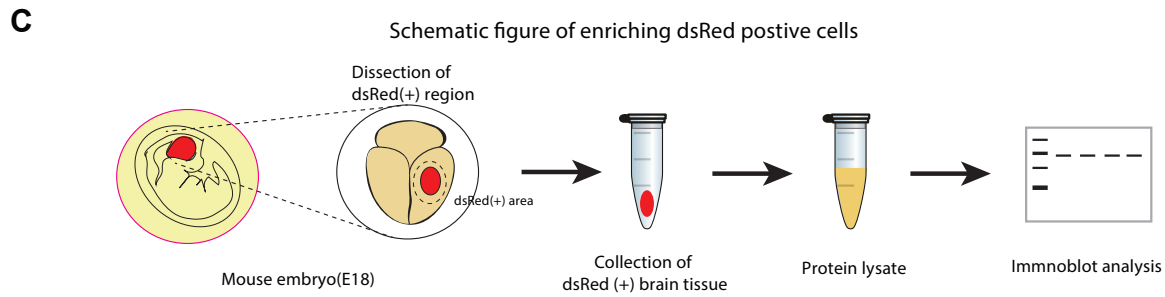
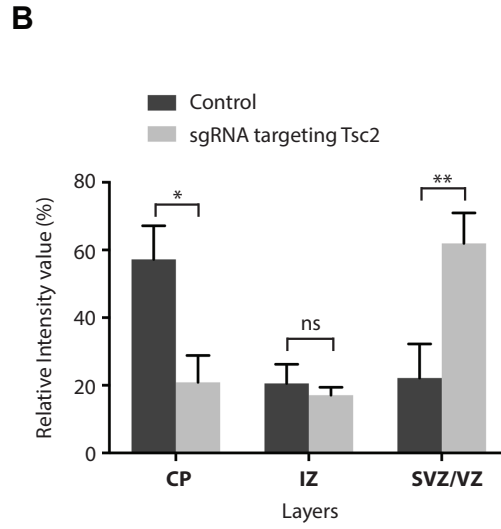
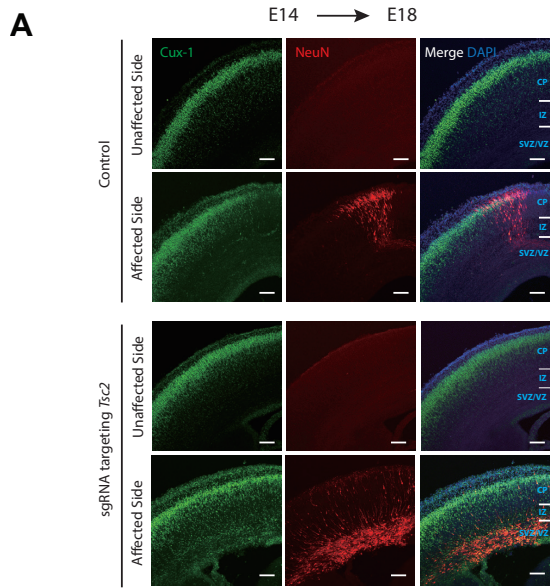
(A-B) 2. Neuro2A cells without Cas9 and sgRNA served as the control parental cells. TSC1 and TSC2 were not detected, suggesting each gene were knocked out using the CRISPR-Cas9 system; the level of phosphorylated S6 increased robustly in both stable cell lines, indicating that mTOR pathway was hyperactivated by disrupting the TSC complex.



**Figure S10.** Schematic showing the procedure of *in utero* electroporation at E14 followed by analysis of the brain coronal sections at E18 or after P56.

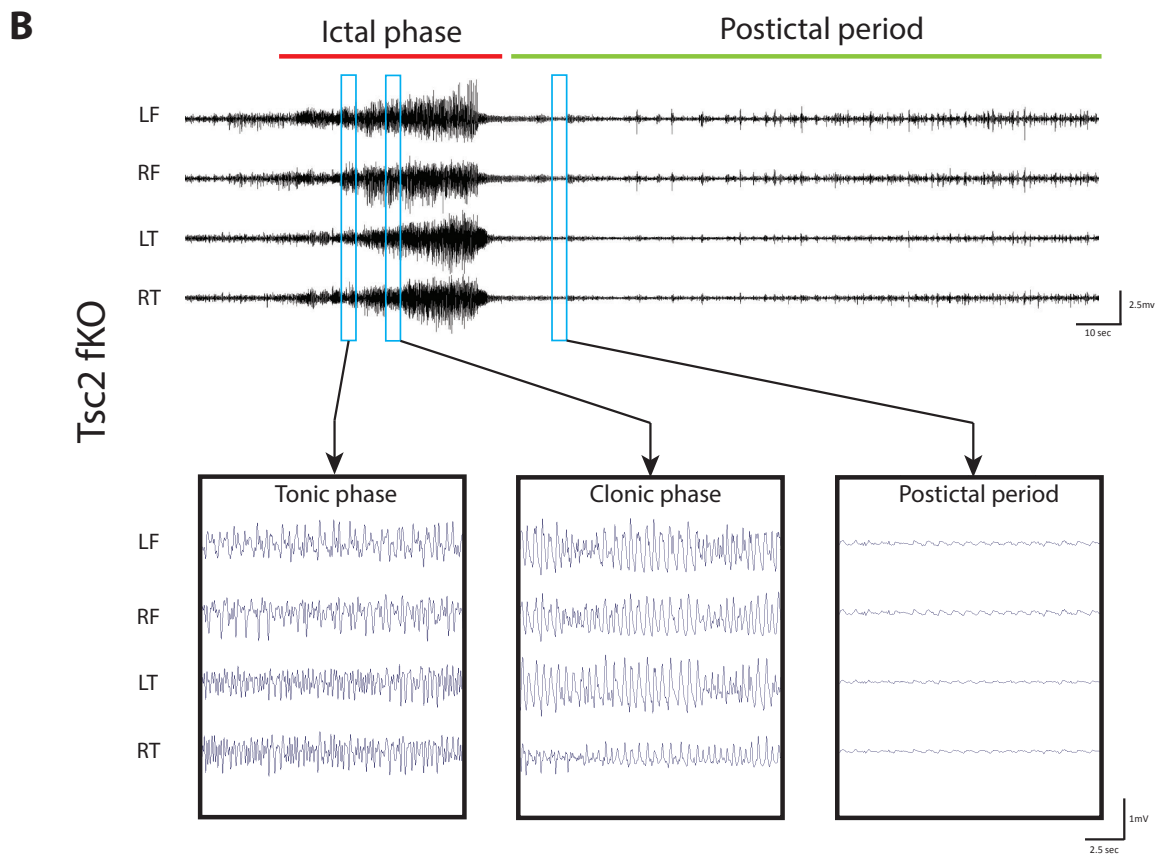
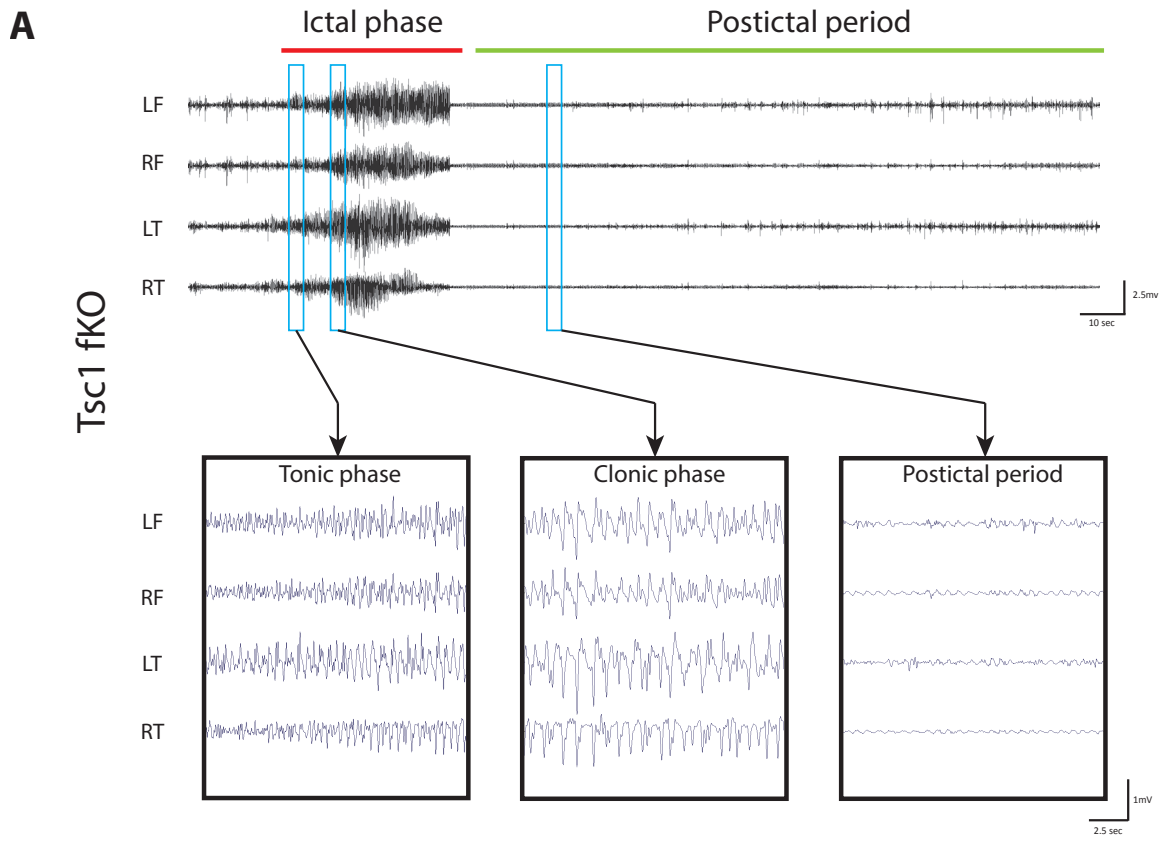
We electroporated *Tsc1* or *Tsc2* targeted CRISPR-Cas9 constructs (sgRNA-Cas9-IRES-mCherry vector) with a dsRed reporter vector (pCAG-dsRed) into the developing mouse brain at embryonic day (E) 14. Then, we dissected the brain at E18 or postnatal day (P) >56 for subsequent analysis such as migration analysis, colocalization analysis and cell size analysis.





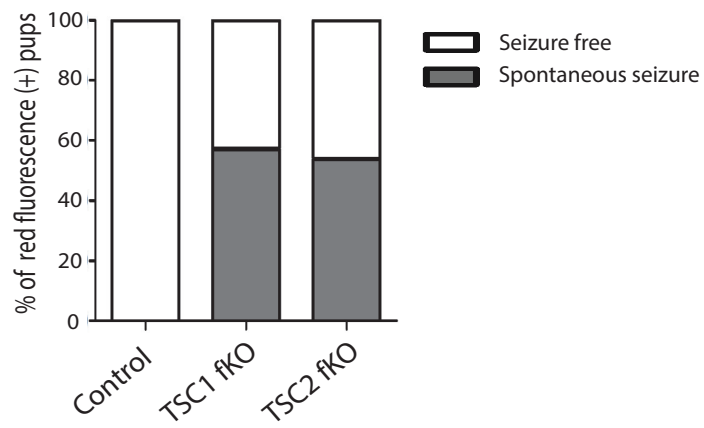
**Figure S11.** The CRISPR construct targeting *Tsc2* is sufficient to disrupt neuronal migration and significantly reduce the expression level of TSC2 protein during the early brain developmental period.

(A) *In utero* electroporation of the CRISPR-Cas9 construct targeting *Tsc2* (sgRNA-Cas9-IRES-mCherry vector) disrupts neuronal migration in the developing mouse neocortex. The images show coronal sections of mouse brains at E18 electroporated with the CRISPR construct. Electroporated mice without sgRNA expression served as the control. Scale bar, 100  $\mu\text{m}$ . (B) The bar charts show the relative fluorescence intensities reflecting the distribution of electroporated cells within the cortex. Data are the mean  $\pm$  SEM (n=5-6 per group). \* $P$ <0.05 and \*\* $P$ <0.01 compared with control, two-way ANOVA with Bonferroni's multiple comparison test. CP, cortical plate; IZ, intermediate zone; SVZ/VZ, subventricular and ventricular zone (C) Schematic figure of enriching dsRed-positive cells in brain tissue. We resected dsRed-positive region of embryonic brain with scalpel and extracted protein lysates for subsequent immunoblot analysis. (D) Immunoblotting for TSC2 and  $\alpha$ -tubulin in the embryonic brain lysate with enriched dsRed-positive cells. The TSC2 level was significantly decreased, suggesting that target gene was properly knockout. (E) Quantification of the blotting intensity. Data are the mean  $\pm$  SEM (n=3 per group). \* $P$ <0.05, Student's t-test. (F) The CRISPR construct targeting *Tsc2* induces the increase of mTOR activity in the developing mouse neocortex. Phosphorylation of S6 protein is significantly increased in dsRed-positive cells carrying CRISPR construct targeting *Tsc2*. (G) Co-localization analysis is performed using Pearson's correlation coefficient and Mander's overlap coefficient. Data are the mean  $\pm$  SEM (n=6~7 per group). \*\*\* $P$ <0.001, Student's t-test., Scale bar, 20  $\mu\text{m}$ .



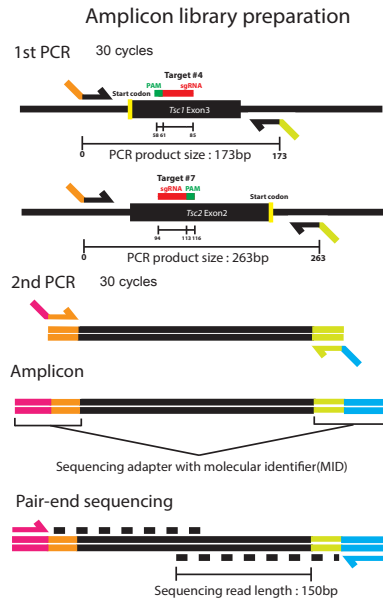
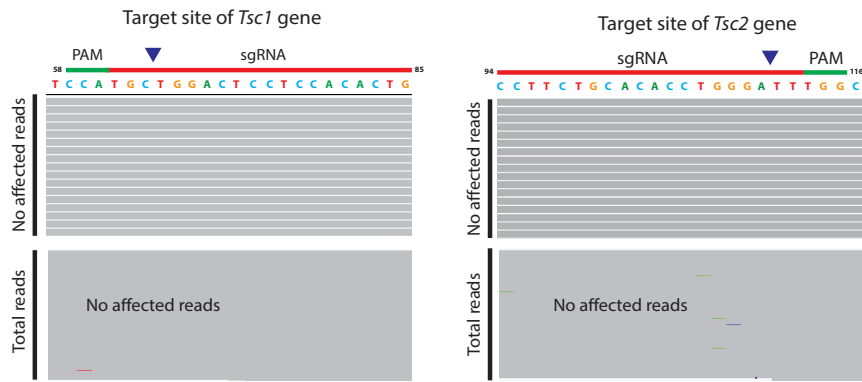
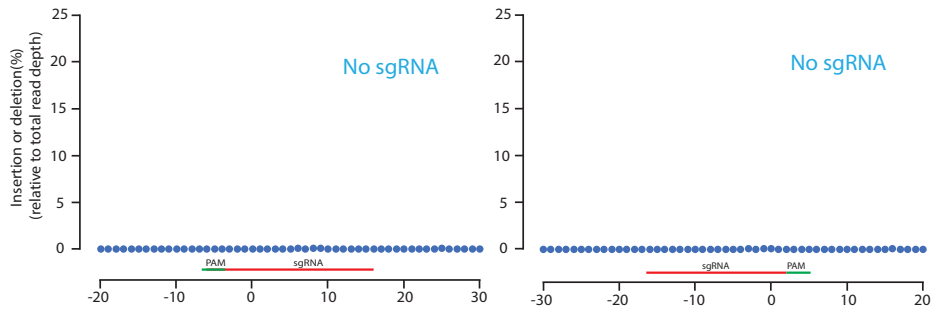
**Figure S12.** EEG wave pattern analysis of the ictal phase and postictal period.

(A-B) The *Tsc1* and *Tsc2* fKO mice showed generalized tonic-clonic seizures consisting of 2 phases (tonic, clonic), followed by postictal attenuation. During the tonic phase, a low amplitude and fast spike were observed with all electrodes, and these waves evolved to exhibit relatively high amplitudes with a spike-wave pattern during the clonic phase. In the postictal period, the wave pattern displayed a diffused attenuation of amplitude. The wave patterns for the EEG signals were recorded from 4 epidural electrodes located on the left frontal lobe (LF), right frontal lobe (RF), left temporal lobe (LT), and right temporal lobe (RT).



**Figure S13.** The percentage of mice showing spontaneous seizure after in utero application of the CRISPR-Cas9 system.

Mice showing spontaneous seizures were counted by video-EEG recording (12h per d for > 2 d). n= 6-14 per group.

**A****B****C**

**Figure S14.** The process used for deep amplicon sequencing of CRISPR-Cas9 targeted *Tsc1* and *Tsc2* sites in microdissected cells.

(A) Schematic figure showing the amplicon sequencing process. A two-step PCR protocol was used to amplify amplicons from genomic DNA that contained a molecular identifier (MID) surrounding the predicted cutting site of Cas9. Paired-end sequencing of the amplicon libraries was performed. (B) Integrative Genomic Viewer showing the deep sequenced *Tsc1* and *Tsc2* sites in isolated dsRed- positive neurons from CRISPR-Cas9 electroporated mice without sgRNA expression (control mice). The arrowhead indicates the theoretical cutting site of Cas9. PAM, protospacer adjacent motif. (C) The frequency (relative to total reads) and position of indels are shown. The '0' position indicates the theoretical cutting site of Cas9 guided by sgRNA.

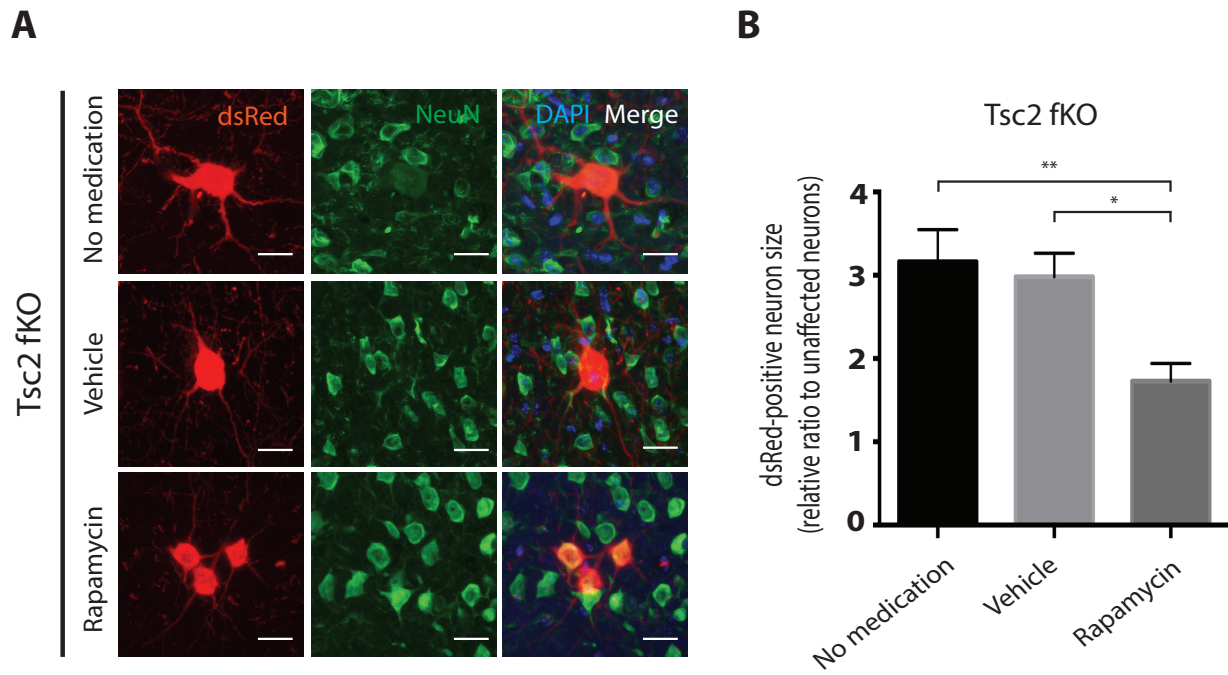


**Figure S15.** Cytomegalic neurons induced by CRISPR construct targeting *Tsc2* are rescued by rapamycin treatment.

(A) Co-immunostaining for NeuN and DAPI. The soma size of dsRed positive neurons was measured. (B) Bar chart of neuronal size in each group in affected cortical regions. The increased soma size was rescued by rapamycin treatment. Data are the mean  $\pm$  SEM (n=32-35 per group). \* $P$ <0.05 and \*\* $P$ <0.01, compared with dsRed-negative neurons, one-way ANOVA with Bonferroni's post-test. Scale bars, 20  $\mu$ m.

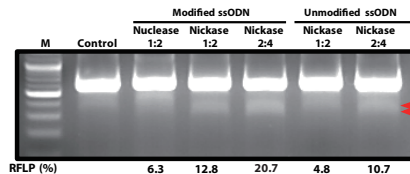
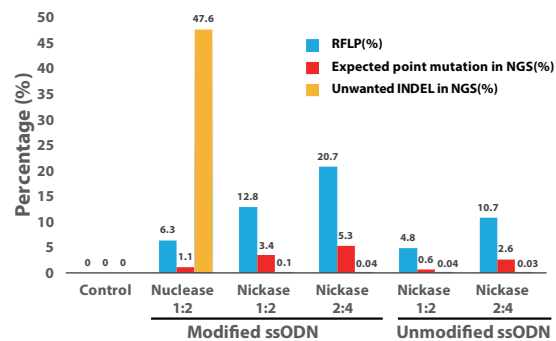


**A**

Wild type  
 TCA GTA CAG CTG CTT GAC CAG ATT CCA TCC TAT GAC ACT  
 CAC AAG ATT GCT GTC CTG TAT GTG GGA GAA GGC CAG GTA  
 AGG CCC TGG GGT CAG CAT AGG ACT

Tsc2 G to A ssODN  
 (Unmodified)  
 TCA GTA CAG CTG CTT GAC CAG ATT CCA TCA TAT GAC ACT  
 CAC AAG ATT GCT **ATA** CTA TAC GTA GGA GAA GGC CAG GTA  
 AGG CCC TGG GGT CAG CAT AGG ACT

Tsc2 G to A ssODN  
 (Modified)  
 T\*C\*A\* GTA CAG CTG CTT GAC CAG ATT CCA TCA TAT GAC ACT  
 CAC AAG ATT GCT **ATA** CTA TAC GTA GGA GAA GGC CAG GTA AGG  
 CCC TGG GGT CAG CAT AGG \*A\*C\*T

**B****C**

**Figure S16.** Comparison of homology-directed repair (HDR) efficiency of modified and unmodified ssODN with Nuclease and Nickase for *Tsc2* c.4576G>A (p.Val1526Ile) using RFLP assay and deep sequencing.

(A) Schematic sequence of the 102-mer ssODN's. Wild-type sequence showing guide sequence (italic and underlined letters) and PAM (red and bold letters). 102-mer unmodified and modified ssODN's which includes several silent mutations which are represented in bold purple letters and point mutation is represented in bold red letter. A NdeI restriction enzyme site was incorporated near to guide sequence, is represented in italic and underlined letters, which is absent at the wild type sequence. In 102-mer phosphorothioate modified ssODN which is represented in asterisk at both sides of 5' and 3' end of the ssODN. (B) RFLP-based analysis in Neuro2A cells, the genomic DNA isolated from different transfected conditions of modified and unmodified ssODN with Nuclease and Nickase pooled cells was subjected to the PCR. PCR amplicons were digested with NdeI in an RFLP assay to detect sequences that resulted from homology-directed repair. Arrowheads indicate the expected position of DNA bands cleaved by NdeI digestion. Untransfected cells were used as the negative control. (C) Deep sequencing (NGS) analysis for transfected Neuro2A cells, the graph showing the efficiency of each experimental set.

The set of Nickase & modified ssODN (2:4 ratio) showed the highest percentage of expected point mutation without unwanted indel.

## Supplemental tables

**Table S1.** Molecular genetic information of FCDII individuals enrolled in this study

See the attached excel file Table\_S1.xlsx.

**Table S2.** \*Clinical findings related to TSC under the guidance of surveillance recommendations for suspected TSC

Individuals	<sup>a</sup> Genetics	<sup>b</sup> Brain	<sup>c</sup> Kidney	<sup>d</sup> Lung	<sup>e</sup> Skin	<sup>f</sup> Teeth	<sup>g</sup> Heart	<sup>h</sup> Eye
FCD64	No findings	No findings	No findings	No findings	No findings	No findings	No findings	No findings
FCD81	No findings	No findings	No findings	No findings	No findings	No findings	No findings	No findings
FCD94	No findings	No findings	No findings	No findings	No findings	No findings	No findings	No findings
FCD98	No findings	No findings	No findings	No findings	No findings	No findings	No findings	No findings
FCD123	No findings	No findings	No findings	No findings	No findings	No findings	No findings	No findings

\*Tuberous Sclerosis Complex Surveillance<sup>3</sup>.

<sup>a</sup>Findings for germline TSC1/2 mutations

<sup>b</sup>Findings for cortical tuber, subependymal nodule, subependymal giant cell astrocytoma or cerebral white matter radial migration lines

<sup>c</sup>Findings for renal angiomyolipoma or multiple renal cysts

<sup>d</sup>Findings for lymphangiomyomatosis

<sup>e</sup>Findings for facial angiofibromas, forehead plaque, unguis fibroma, hypomelanotic macules, shagreen patch or "Confetti" skin lesions

<sup>f</sup>Findings for multiple pits in dental enamel, gingival fibromas

<sup>g</sup>Finding for cardiac rhabdomyoma

<sup>h</sup>Findings for multiple retinal nodular hamartomas or retinal achromic patch

**Table S3.** Summary of mutation calls in saliva samples from individuals carrying mutation in this study

Patient ID	Gene	Nucleotide changes	Protein changes	Hybrid capture sequencing				
				Tissue	Platform	% Mutant allele	Ref. count	Mut. Count
FCD064	TSC1	c.610C>T	p.Arg204Cys	Saliva	hybrid Capture	0.12	2605	3
FCD081	TSC1	c.64C>T	p.Arg22Trp	Saliva	hybrid Capture	0.00	122	0
FCD094	TSC2	c.4639G>A	p.Val1547Ile	Saliva	hybrid Capture	0.00	239	0
FCD098	TSC1	c.64C>T	p.Arg22Trp	Saliva	hybrid Capture	NA	NA	NA
FCD123	TSC1	c.64C>T	p.Arg22Trp	Saliva	hybrid Capture	0.44	2709	12
Patient ID	Gene	Nucleotide changes	Protein changes	PCR amplicon Sequencing				
				Tissue	Platform	% Mutant allele	Ref. count	Mut. Count
FCD064	TSC1	c.610C>T	p.Arg204Cys	Saliva	Amplicon	NA	NA	NA
FCD081	TSC1	c.64C>T	p.Arg22Trp	Saliva	Amplicon	NA	NA	NA
FCD094	TSC2	c.4639G>A	p.Val1547Ile	Saliva	Amplicon	NA	NA	NA
FCD098	TSC1	c.64C>T	p.Arg22Trp	Saliva	Amplicon	NA	NA	NA
FCD123	TSC1	c.64C>T	p.Arg22Trp	Saliva	Amplicon	NA	NA	NA

The following abbreviation is used: Ref, reference, Mut, mutation

**Table S4.** Summary of mutation calls in brain samples from individuals carrying mutation in this study

Patient ID	Replication	Gene	Nucleotide changes	Protein changes	Hybrid capture sequencing				
					Tissue	Platform	% Mutant allele	Ref. count	Mut. Count
FCD064	Biological,Crossplatform	TSC1	c.610C>T	p.Arg204Cys	Brain FFPE	hybrid Capture	1.75	225	4
FCD081	Biological,Crossplatform	TSC1	c.64C>T	p.Arg22Trp	Brain FFPE	hybrid Capture	2.81	173	5
FCD094	Biological,Crossplatform	TSC2	c.4639G>A	p.Val1547Ile	Brain FFPE	hybrid Capture	1.19	414	5
FCD098	Biological,Crossplatform	TSC1	c.64C>T	p.Arg22Trp	Brain FFPE	hybrid Capture	2.52	155	4
FCD123	Biological,Crossplatform	TSC1	c.64C>T	p.Arg22Trp	Brain FFPE	hybrid Capture	2.21	264	6
Patient ID	Replication	Gene	Nucleotide changes	Protein changes	PCR amplicon Sequencing				
					Tissue	Platform	% Mutant allele	Ref. count	Mut. Count
FCD064	Biological,Crossplatform	TSC1	c.610C>T	p.Arg204Cys	Brain FFPE	Amplicon	1.00	2375.00	24.00
FCD081	Biological,Crossplatform	TSC1	c.64C>T	p.Arg22Trp	Brain FFPE	Amplicon	2.00	441	9
FCD094	Biological,Crossplatform	TSC2	c.4639G>A	p.Val1547Ile	Brain FFPE	Amplicon	1.55	254.00	4.00
FCD098	Biological,Crossplatform	TSC1	c.64C>T	p.Arg22Trp	Brain FFPE	Amplicon	1.98	1038	21
FCD123	Biological,Crossplatform	TSC1	c.64C>T	p.Arg22Trp	Brain FFPE	Amplicon	1.37	794	11

The following abbreviation is used: Ref, reference, Mut, mutation

**Table S5.** Summary of mutation calls from all tested patients in this study

See the attached excel file Table\_S5.xlsx.

**Table S6.** Functional annotations for detected missense mutations

Patients	Detected Gene	dbSNP(common)	Nucleotide change	Amino acid change	polyPhen	Grantham	PhastCons	GERP	SIFT
FCD64	TSC1	none	c.610C>T	p.Arg204Cys	1	180	1	6.08	0(damaging)
FCD81	TSC1	none	c.64C>T	p.Arg22Trp	0.999	101	0.928	3.21	0.04(damaging)
FCD94	TSC2	none	c.4639G>A	p.Val1547Ile	0.998	112	0.978	4.45	0.04(damaging)
FCD98	TSC1	none	c.64C>T	p.Arg22Trp	0.999	101	0.928	3.21	0.04(damaging)
FCD123	TSC1	none	c.64C>T	p.Arg22Trp	0.999	101	0.928	3.21	0.04(damaging)

**Table S7.** List of oligonucleotides used for sgRNA construction

Gene	Targets	Direction	Sequence (5' to 3')
<i>Tsc1</i>	T1	FP	CCGGCTCCCAATGTTGGCTAACT
		RP	AAACAGTTAGCCAACATTGGGGAG
	T2	FP	CCGGGGAGAGCAGCTCCCAATGT
		RP	AAACACATTGGGGAGCTGCTCTCC
	T3	FP	CCGGGGCCAGTTAGCCAACATTG
		RP	AAACCAATGTTGGCTAACTGGGCC
	T4	FP	CCGGCAGTGTGGAGGAGTCCAGCA
		RP	AAACTGCTGGACTCCTCCACACTG
	T5	FP	CCGGTGGGGAGCTGCTCTCCATGC
		RP	AAACGCATGGAGAGCAGCTCCCA
	T6	FP	CCGGATCCCGCACACCCAGTGTGG
		RP	AAACCCACACTGGGTGTGCGGGAT
	T7	FP	CCGGATGCTGGACTCCTCCACACT
		RP	AAACAGTGTGGAGGAGTCCAGCAT
	T8	FP	CCGGCTCCTCCACACTGGGTGTGC
		RP	AAACGCACACCCAGTGTGGAGGAG
	T9	FP	CCGGATTGAGGGACTCCTTGAAGA
		RP	AAACTCTTCAAGGAGTCCCTCAAT
	T10	FP	CCGGTGACGTGACAGCCATCTTCA
		RP	AAACTGAAGATGGCTGTCACGTCA
<i>Tsc2</i>	T1	FP	CCGGAAGCCGGAATCTTTGCTTGT
		RP	AAACACAAGCAAAGATTCCGGCTT
	T2	FP	CCGGCTTGAACTTCTCCTTCAAGC
		RP	AAACGTTGAAGGAGAAGTCAAG
	T3	FP	CCGGAACAACAAGCAAAGATTC
		RP	AAACGAATCTTTGCTTGTGGTTT
	T4	FP	CCGGAAGCAAAGATTCCGGCTTGA
		RP	AAACTCAAGCCGGAATCTTTGCTT
	T5	FP	CCGGGAGAAGTTCAAGATACTGTT
		RP	AAACAACAGTATCTTGAACTTCTC
	T6	FP	CCGGTGTGGGATTGGGAACATCG
		RP	AAACCGATGTTCCAATCCAACA
	T7	FP	CCGGCCTTCTGCACACCTGGGATT
		RP	AAACAATCCCAGGTGTGCAGAAGG
	T8	FP	CCGGTGTTCCTTCTGCACACCT
		RP	AAACAGGTGTGCAGAAGGCAAACA
	T9	FP	CCGGGAACATCGAGGCCAAATCCC
		RP	AAACGGGATTTGGCCTCGATGTTC
	T10	FP	CCGGCCAAATCCCAGGTGTGCAGA
		RP	AAACTCTGCACACCTGGGATTTGG

FP: forward primer, RP: Reverse primer

**Table S8.** The sequence of primers used in the T7E1 assay

Gene	Direction	Sequence (5' to 3')
<i>Tsc1</i>	FP	GCTCTTCCCACTTGAGCCATT
	RP	CAACACCATGCCTGACTGGA
	FP1	AAGCAGAGAGAACGACTCCCA
	RP1	TCTGTTCACAGCAAGAAAACCC
<i>Tsc2</i>	FP	GGTGAGGGGAATTGGTCGTT
	RP	GGAGGACCCAGTCTCACTACT
	FP1	TTCAAGCCCTCCATTGCGAA
	RP1	CGTGCTGAGAGAGTACAGGG

FP: forward primer, RP: Reverse primer

**Table S9.** The sequence of oligonucleotides used in targeted deep sequencing

Primer		Sequence(5'-3')
<b>Primers 1 for RFLP assay</b>	FP	GGTCCTTGGCCGTAGAGTTT
	RP	CCGGCATTAAATAACGGTGGC
<b>Primers 2 for RFLP assay</b>	FP	CAGCTCTACCATTGCGCCCTT
	RP	ACCCTCTGTCCTGCCACTTA
<b>Region-specific primers for deep sequencing</b>	FP	ACACTCTTTCCTACACGACGCTCTTCCGATCT CTGTCTGGGTTGGTGGCTG
	RP	GTGACTGGAGTTCAGACGTGTGCTCTTCCGATCT CTCTGACCTACTGCTGAGCC
<b>Primers for Illumina indexing</b>	FP	AAT GAT ACG GCG ACC ACC GAG ATC TAC AC (8bp barcode) ACA CTC TTT CCC TAC ACG AC
	RP	CAA GCA GAA GAC GGC ATA CGA GAT (8bp barcode) GTG ACT GGA GTT CAG ACG TGT

FP: forward primer, RP: Reverse primer

**Table S10.** The sequence of primers and probes used in ddPCR

Target	Category	Sequence (5' to 3')
<b>TSC1 R22</b>	Forward primer	GTGGCTCTAAAGTCAATCTCTTCT
	Reverse primer	CTTCTTGCCATGCTGGACT
	Probe targeting G allele	/5HEX/T+G+C+GGG+A+CGA/3IABkFQ/
	Probe targeting A allele	/56-FAM/T+G+T+GGGA+C+GA/3IABkFQ/
<b>TSC2 V1547</b>	Forward primer	CCTCGACCAGATCCCATCATA
	Reverse primer	CCCTGTCCAGGCACCTA
	Probe targeting G allele	/5HEX/C+AGG+A+C+GGC+GA/3IABkFQ/
	Probe targeting A allele	/56-FAM/AC+AGG+A+T+GGC+GA/3IABkFQ/

+ : locked nucleic acid (LNA)

### Supplemental References

1. Cingolani, P., Platts, A., Le Lily Wang, Coon, M., Nguyen, T., Wang, L., Land, S.J., Lu, X., and Ruden, D.M. (2012). A program for annotating and predicting the effects of single nucleotide polymorphisms, SnpEff. *Fly* 6, 80–92.
2. Kuilman, T., Velds, A., Kemper, K., Ranzani, M., Bombardelli, L., Hoogstraat, M., Nevedomskaya, E., Xu, G., de Ruiter, J., Lolkema, M.P., et al. (2015). CopywriteR: DNA copy number detection from off-target sequence data. *Genome Biol.* 16, R163–15.
3. Northrup, H., Krueger, D.A., International Tuberous Sclerosis Complex Consensus Group (2013). Tuberous sclerosis complex diagnostic criteria update: recommendations of the 2012 International Tuberous Sclerosis Complex Consensus Conference. pp. 243–254.